Journal of Molecular Catalysis A: Chemical 322 (2010) 17–25

Contents lists available at ScienceDirect

Journal of Molecular Catalysis A: Chemical

journal homepage: www.elsevier.com/locate/molcata

Some optimization in preparing core-shell Pt–ceria catalysts for water gas shift reaction

Connie Mei Yu Yeung, Shik Chi Tsang*

Wolfson Catalysis Centre, Inorganic Chemistry Laboratory, University of Oxford, Oxford OX1 3QR, UK

ARTICLE INFO

Article history:
Received 8 February 2009
Received in revised form 7 January 2010
Accepted 1 February 2010
Available online 6 February 2010

Keywords:
Microemulsion
WGS
Noble metal
Ceria
Interface
Co-addition
Sequential addition
Core-shell

ABSTRACT

Pt on ceria-based catalysts have been extensively investigated in recent years since they could be promising alternatives to Cu-based catalysts for hydrogen production from water gas shift reaction. A core-shell Pt in thin layer ceria prepared by microemulsion technique has earlier been shown to be highly active and selective for WGS reaction as compared to those Pt–ceria catalysts prepared by traditional methods. This paper is to report some optimization parameters including the sequence of adding precursors, aging time, type of reducing agent, support effect, variation in metal core composition and substitution of cerium oxide with other lanthanum metal ions in preparation of desirable metal-support interface for the catalysis. It is reported that a bimetallic core of Pt and Au in a 1:1 ratio at 5 wt% with respect to the ceria shell shows the highest WGS activity. Doping of rare earth metal ions to the ceria coating in the platinum–gold encapsulated does not result in a higher activity. This suggests that the overall catalytic WGS activity of this type of catalysts depends on electronic aspect of metal–ceria interface instead of oxygen mobility and OSC properties of the promoted ceria oxide shell.

1. Introduction

There is a renewed interest in the catalysed water gas shift reaction, WGS ($CO + H_2O \rightleftharpoons CO_2 + H_2$) for the purification of H_2 rich feeds obtained through hydrocarbon reforming. H_2 is seen as the key fuel for future power generation using for both stationary and mobile applications. The use of WGS reactors with small-scale reformers imposed different requirements compared to large-scale H_2 production plants, which are based on commercial $Cu/ZnO/Al_2O_3$ catalyst technology. Noble metal (NM)/ceria-based catalysts have been extensively investigated in recent years [1–8] for the WGS reaction ($CO + H_2O \rightleftharpoons CO_2 + H_2$) in order to produce more H_2 rich feeds from reformate mixtures. In terms of volume produced, hydrogen is by far the most important component. For the majority of energy and chemical applications, hydrogen must be of high purity, and carbon oxides, in particular carbon monoxide (a strong catalyst poison), must be reduced to very low levels (ppm) [9]. In the case of mobile applications, particularly pure hydrogen is required to supply to the PEM fuel cells close to their operation temperatures for efficient heat management. Thus, there is tremendous interest to identify active WGS catalysts at temperatures around 80–150 °C regime. However, for stationary applications, production of pure hydrogen for the manufacture of fine chemicals at small scale is in significant demand. Higher temperature is desirable since reaction kinetics would be more favorable but the WGS thermodynamic equilibrium position tends to shift to the CO/H_2O direction. Thus, a compromise in operation temperature to obtain fast kinetics and high purity hydrogen feed is needed. Currently, hydrogen production at large industrial scale employs two stage processes, Fe–Cr oxide catalyst for high temperature WGS reaction (310–450 °C) and a $Cu/ZnO/Al_2O_3$ catalyst for low temperature WGS reaction (210–240 °C) under steady-state conditions. This commercial process is rather engineering cumbersome and is not well suited for a small-scale hydrogen production. In particular, the large reactor volume dictated by the slow WGS kinetics of the Cu/ZnO catalyst at low temperatures is an obstacle that hinders its application in fuel processing. Thus, developing a more active NM/ceria-based catalyst over the less active Cu-based catalyst technology used in small WGS reactors for low temperature mobile (fuel cells) applications and for high temperature stationary application is currently under intense investigation. Ceria, CeO_2, has been identified as one potential important catalyst component for the LT hydrogen production from WGS [10]. Pure ceria is well known to store and release oxygen and hydrogen, *via* forming surface and bulk vacancies or inter-metallic M–Ce compounds. Ceria can also serve as a stabilizer to metal and alumina supports maintaining a high dispersion of the catalytic metals [11–13]. In addition, ceria can be used as a promoter in combination with other elements to give mixed-oxide formulations. Cerium oxide-containing WGS formulations have therefore attracted considerable interest from catalyst manufacturers [14]. As

* Corresponding author. Tel.: +44 1865282610; fax: +44 1865272659.
E-mail address: edman.tsang@chem.ox.ac.uk (S.C. Tsang).

1381-1169/$ – see front matter © 2010 Elsevier B.V. All rights reserved.
doi:10.1016/j.molcata.2010.02.001

a result, metal–ceria WGS catalysts have been developed as potentially better alternatives to the HT applicable pyrophoric Cu–ZnO. For example, Li [15] reported that copper or nickel on $Ce(La)O_x$ catalysts prepared by urea precipitation–gelation displayed good LT shift activity at high space velocities when tested under low CO concentrations (2%). They attributed the high activity of their catalyst to the enhanced reducibility of ceria in the presence of the metal. Ruettinger [16] developed a base metal non-pyrophoric particulate catalyst with a very promising catalytic behavior with respect to the requirements of fuel cell applications. This catalyst only showed a very slight temperature increase of 40 °C without any deactivation if it was (accidentally) exposed to air. Lost activity due to liquid water exposure was shown to be regenerated *in situ* or *ex situ*. Perhaps, one most significant earlier result came from Swartz [17] who reported that Pt/CeO_2 catalyst was non-pyrophoric but showed much high activity than Cu-based catalysts at a high space velocity. Recently, gold-particles supported on CeO_2 [18,19] have been reported to be highly active for the WGS, with their improved activity at low temperature being explained as due to the synergism of the gold–metal oxide.

In addition, much of the research in this area reported in the literature has involved the use of an artificial gas mixture (CO/H_2O) for the WGS study rather than the use of reformate which contains high levels of hydrogen and carbon dioxides. The effects of these gas mixtures on the WGS reaction are not yet clear over the NM/ceria catalysts, though the direct use of reformate would be practically more relevant than using an artificial gas mixture. One immediate technical problem is that at high levels of hydrogen and carbon oxides, other side reactions could also be simultaneously taking place during the WGS catalysis. For example, the methanation reactions:

$$CO_{(g)} + 3H_{2(g)} \rightleftharpoons CH_{4(g)} + H_2O_{(g)}, \quad \Delta H^\circ_{298} = -205\ \text{kJ mol}^{-1} \qquad \text{Reaction 1}$$

$$CO_{2(g)} + 4H_{2(g)} \rightleftharpoons CH_{4(g)} + 2H_2O_{(g)}, \quad \Delta H^\circ_{298} = -165\ \text{kJ mol}^{-1} \qquad \text{Reaction 2}$$

These side reactions are known to be unimportant over the traditional Cu or Cr based WGS catalysts, since the C–O bond is likely to remain intact (associative adsorption of CO) before it is converted into CO_2 during the WGS. However, NMs are able to dissociatively adsorb CO leading to the breakage of C–O linkage on their surfaces, hence favoring the formation of methane and higher hydrocarbons under hydrogen rich conditions. In fact, a significant quantity of methane and high hydrocarbons has indeed been detected during the WGS study over the NM/ceria (prepared by traditional methods) by workers at Synetix, Johnson Matthey [20]. Thus, the high selectivity for the WGS reaction is required over the competing reactions of methanation as these can lower the H_2 content of the final feed.

In our previous communications, we reported that the new class of microemulsion prepared NM/ceria catalysts which show a comparable or even higher catalytic activity towards the WGS reaction than those catalysts prepared by traditional methods [21,22]. Our preliminary observation was that this new type of catalysts also inhibits methane formation at elevated temperatures.

In this paper, we will present some optimization studies for the synthesis of microemulsion prepared NM/ceria catalysts for WGS reaction and a discussion on the establishment of active interface between metal and ceria using microemulsion as compared to those catalysts prepared by traditional methods will be included.

2. Experimental

2.1. Microemulsion (sequential addition) prepared Pt/CeO_2 catalysts

The typical procedure for preparing 5 wt% Pt/ceria catalysts by the microemulsion (MEs) technique is as follows: a cationic surfactant, cetyltrimethylammonium bromide, CTAB was added into dry toluene with vigorous stirring. A water to surfactant ratio, *W*, of 30 was employed in this synthesis. A suspension of CTAB in toluene was formed immediately. Then, the Pt-precursor salt solution with ceria was prepared by dissolving an appropriate amount of $(NH_4)_2PtCl_6$ into the DI water. The aqueous solution of Pt-precursor salt was then added dropwise to the suspension of CTAB in toluene and was stirred overnight. A solution of 0.22 g of sodium hydroxide pre-dissolved in 1.630 mL of DI water was added into the reaction mixture and stirred for 2 h before adding a solution of 0.6060 g of cerium(III) nitrate hexahydrate. It is noted that the final water to surfactant molar ratio of the resulting mixture was maintained at 30 as in the MEs method. The reaction mixture was aged for 6 days with constant stirring. After the ageing step, the reaction mixture was centrifuged for 20 min at 1000 rpm in order to collect the product. The product was then washed with EtOH at least four times to remove surfactants. The solution was repeatedly centrifuged after each washing. The solid product obtained was dried overnight in air. The catalysts were then pre-treated with the reactant gas mixture (8% CO, 10% CO_2, 1% CH_4, 32.5% H_2 balancing with N_2) at 400 °C before catalytic testing.

2.2. Co-precipitation prepared Pt/CeO_2 catalyst

2 wt% Pt/ceria catalysts synthesised by the co-precipitation method were prepared as follows. 0.1541 g of ammonium tetrachloroplatinate(II), $(NH_4)_2PtCl_4$, was dissolved in a 100 mL aqueous solution of 0.2 M cerium(III) nitrate hexahydrate, $Ce(NO_3)_3{\cdot}6H_2O$, and sprayed into a 250 mL ammonia solution under a constant stirring. The precipitate was allowed to age at room temperature with stirring for another 2 h. Then, it was collected by centrifugation at 1000 rpm and washed twice with water and once with ethanol to remove any remaining ammonia and reaction by-product. The solid was dried at 60 °C in a vacuum oven for 2 h. Then, it was dried in a flowing stream of nitrogen at 100 mL min^{-1} at a temperature ramp of 2 °C min^{-1} from room temperature to 350 °C and then held for further 5 h. After the drying procedure, it was pre-reduced with 50 mL min^{-1} hydrogen at programming of 2 °C min^{-1} up to 250 °C and held for further 3 h.

2.3. Wet impregnation prepared Pt/CeO_2 catalyst

5 wt% Pt/ceria catalysts synthesized by wet impregnation were prepared as follows. Cerium(III) nitrate hexahydrate was calcined in static air with temperature programming (25 °C min^{-1}) from room temperature to 600 °C and was held at 600 °C for a further 10 h. Ammonium tetrachloroplatinate(II) or hexachloroplatinate(IV) was dissolved in DI water. The Pt-precursor solution was then wet impregnated onto the calcined ceria. The product was dried under air with temperature programming (5 °C min^{-1}) from room temperature to 100 °C and was held at 100 °C for a further 10 h. The catalyst was then calcined in a flowing stream of nitrogen at 30 mL min^{-1} with temperature programming (20 °C min^{-1}) from room temperature to 500 °C and was held for a further 2 h.

3. Results and discussion

First, WGS activity of a catalyst is evaluated as a percent of CO conversion (CO fraction conversion) using 0.77% CH_4, 6.15% CO, 7.68% CO_2, 24.99% H_2, 23.08% H_2O balanced with N_2. Variation in gas hour space velocity using a linear flow rate of 90 mL min^{-1} over different masses of a commercial $Cu/ZnO/Al_2O_3$ supplied by Jonhson Matthey at 300 °C, packed in 4 mm i.d. reactor tube with powder packing density 1 g mL^{-1} was studied as compared to calculated thermodynamic equilibrium CO/CO_2 ratio (CO fraction conversion) under the conditions. It was found that the fraction

Table 1
Comparison of WGS and methanation activities of various catalysts.

Catalyst	CO fraction conversion/%[a]	CH_4 production/%[b]
$Cu/ZnO/Al_2O_3$	55.4	0.03
Co-precipitated 2% Pt/ceria	58.6	13.6
Wet impregnated 5% Pt/ceria	53.2	1.51
MEs – 5% Pt/ceria	62.5	0.0
MEs – 5% Pt, 5% Au/ceria	70.6	0.0

[a] WGS activity is expressed as a percent of CO conversion using 0.77% CH_4, 6.15% CO, 7.68% CO_2, 24.99% H_2, 23.08% H_2O balanced with N_2 at GHSV of 108,000 h^{-1} at 400 °C.
[b] Percent of methane production with respect to the input 0.77% CH_4 at 500 °C.

conversions showed a linear relationship with respect to the mass of catalyst (inverse relationship with GHSV) over our equipment until 735.6 mg where equilibrium value was established. Thus, 50 mg of catalyst with GHSV of 108,000 h^{-1} was selected where the testing conditions was clearly in kinetic control regime. The percent of methane production (a minor reaction from hydrogenation of carbon oxides) is expressed with respect to the input 0.77% CH_4. Table 1 summarizes the CO fraction conversions of WGS reaction at 400 °C and methane production over the various catalysts at 500 °C, respectively [21]. It is noted that the commercial $Cu/ZnO/Al_2O_3$ gives good activity for WGS at comparable temperatures. However, as stated, Cu-based catalysts tend to be pyrophoric on exposure to air after reduction, which were not subjected to further study. Interestingly, the CO fraction conversions over the two Pt/ceria catalysts prepared by microemulsion and co-precipitation show very similar values for the whole temperature range. Their CO fraction conversions also follow closely to the equilibrium line particularly at above 400 °C. However, it is noted that the co-precipitated Pt/ceria gives a significant quantity of methane production (1.01% from *methanation* of carbon oxides on metal surface) from the gas mixture at 500 °C. Equally, the Pt/ceria catalyst prepared by the wet impregnation shows a lower activity towards the WGS due to the low surface area ceria, but it yields a measurable quantity of methane. Addition of gold to platinum in the microemulsion prepared catalyst can also improve the WGS activity with no methane production. These results suggest clearly an interesting fact that the nature of active sites for methanation (known to take place on extended metal ensemble surface [23]) is not the same for WGS giving the possibility of optimising metal containing catalysts for WGS without methane production.

3.1. Morphology of Microemulsion catalyst

The typical NM/ceria catalysts prepared by microemulsion (sequential addition) were characterized by XRD analysis. No platinum metal diffraction was detected (metal size < 2 nm) in all these catalysts with only ceria peaks identified in the spectra. Ceria presented in the sample was also found to be a match to the CeO_2 (Ce(IV)) phase (fluorite structure) in all the samples. The typical XRD spectrum of 5 wt% Pt/ceria prepared by microemulsion is shown in Fig. 1. An estimation of ceria particle size *via* CeO_2 (1 1 1) line broadening from the spectrum with taking instrumental broadening into account shows the ceria particle size of about 3.7 ± 0.5 nm.

Fig. 2 (TEM micrograph) shows the nearly spherical (faceted), highly crystalline ceria particles after calcination, (1 1 1) lattice fringes of 3.12 Å, with each particle 4 ± 1 nm in size with a degree of particle aggregation. Thus, the average ceria size derived from both the XRD and TEM results match with each other. This diameter also agrees well with our previous work with Pt/silica particles prepared with the same W ratio of 30 (which defines the size of emulsion water droplet) [24,25]. Under a careful examination of the TEM

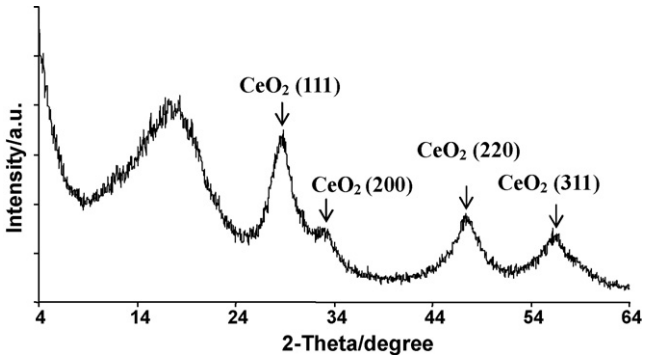

Fig. 1. A typical XRD spectrum of 5 wt% Pt/CeO_2 prepared by microemulsion method.

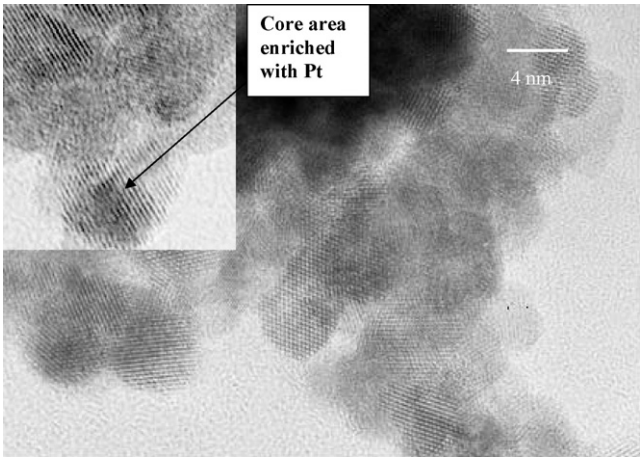

Fig. 2. Transmission electron micrograph (obtained from JOEL 2010) showing ~4 nm spherical ceria particles (3.12 Å lattice fringes corresponding to CeO_2 (1 1 1) is clearly visible) in the ME – 5 wt% Pt/ceria (inset shows the enlarged image of an isolated nanoparticle with Pt enrichment in core area).

micrograph (Fig. 2), the core enriched with Pt (EDX and mapping) is clearly evident inside each ceria particle (content depending on metal precursor content added).

For comparative purpose, 50% Au core in a thick silica coating (particle size of 85 ± 1 nm) were also synthesized using the ME method. Fig. 3 (TEM micrograph) shows the highly spherical Au nanoparticle encapsulated in each silica particle with almost particle aggregation. The TEM image for Au–silica encapsulation appears to be more convincing than for Pt–ceria due to the lack in contrast

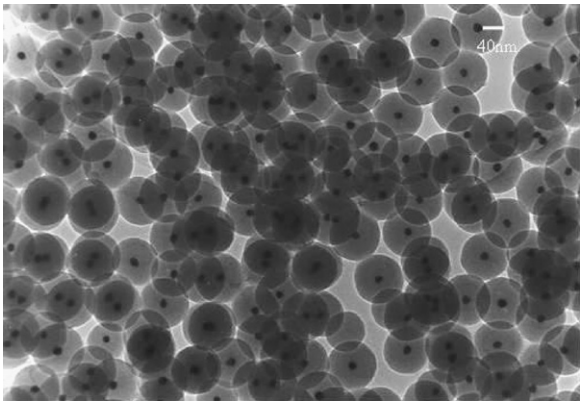

Fig. 3. Transmission electron micrograph (obtained from JOEL 2010) showing relative large silica encapsulated Au particle (50% Au/silica) synthesized by MEs method for comparative purpose.

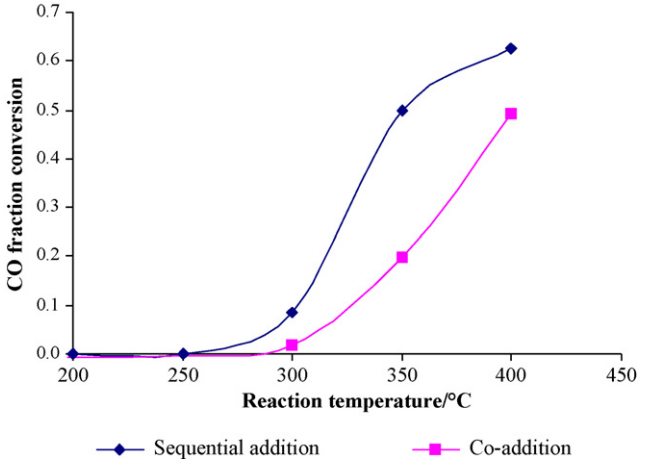

Fig. 4. A plot of CO fraction conversion vs. reaction temperature for WGS reaction over Pt/CeO_2 catalysts with different procedure of adding precursors.

between Ce and Pt. Also, the higher metal content in the core, the thicker but non-crystalline silica over-layer and the propensity of gold forming spherical particle (poor wetting to support) clearly demonstrate that the unique interface/morphology between metal and the encapsulated support prepared by this ME technique.

3.2. Effect of sequence on adding precursor

It is believed that the procedure of adding precursors into the micelles could be important with respect to the geometry of the resulting catalyst. As a result, 5 wt% Pt/CeO_2 was first prepared via adding an aqueous solution of Pt metal precursor ($(NH_4)_2PtCl_6$) followed by adding another aqueous solution containing a ceria precursor into the toluene stabilized microemulsion in a sequential manner (sequential addition). Another catalyst with all the aqueous precursors added at the same time (co-addition) was also prepared. All the post treatments of these two catalyst precursors were identical.

The result of their catalytic activity towards WGS reaction is shown in Fig. 4. The figure clearly suggests that the sample prepared by sequential addition of precursors delivers a much higher activity (62.5%) than the sample with all of the precursors added together (49.2%) at 400 °C. Apart from the difference in the catalytic activity a side product, methanation, was clearly observed (5.6% at 500 °C) in the case of precursor co-addition while no methane production was detected for the sample prepared by the sequential precursor addition.

It is interesting that exceedingly low metal dispersion values (from CO chemisorption) of 0.78% and 3.0% were obtained for the samples prepared by sequential addition and co-addition, respectively. Such a low metal dispersion value (co-precipitation prepared 2% Pt/CeO_2 gives 14.2% Pt metal dispersion) was unusual indicating that most metal sites as a core are totally covered by the cerium oxide (the typical core-shell geometry catalyst prepared by the ME method). The slightly high metal dispersion value (3.0%) in the case of co-addition may reflect a small degree of metal segregation from the core-shell catalyst. This is indeed supported by the above fact that a small quantity of methane (catalytic methanation on CO/H_2 accessible metal surface) was produced over this catalyst.

3.3. Effect of different base used

The effect of using a different base to precipitate platinum and ceria precursors in micelles was studied in this work. 5 wt% Pt/CeO_2 catalysts prepared using the two different bases (sodium hydroxide or ammonia) were tested under the same WGS conditions. The result is shown in Fig. 5. As seen, it is interesting to find that the CO fraction conversions over the temperature range for both catalysts are very different. In particular, the on-set activity of the sample using sodium hydroxide takes off at a lower temperature (higher activity) than that one using ammonia. Also, methane production (indicative of metal exposure) for the sample prepared using ammonia was nearly six times that of the sample using sodium hydroxide as a base (30.3% vs. 5.1% at 500 °C). It is interesting that from the XRD line broadening, the calculated particle size of ceria in the sample using ammonia (5.5 ± 0.5 nm) exceeded that of the micelle synthesized particle size (3.3 ± 0.5 nm).

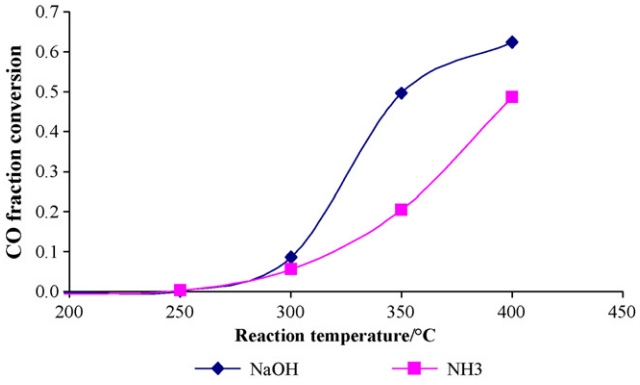

Fig. 5. A plot of CO fraction conversion vs. reaction temperature over Pt/CeO_2 catalysts with different base used to precipitate Pt and ceria towards WGS reaction.

It is anticipated that different bases may affect polymerization of cerium hydroxyl species to form ceria in a reversed micelle during the ageing process, hence affecting the geometry of metal encapsulation in ceria. In addition, the pH value in the reversed micelle could determine the surface charge of ceria. One key issue for the successful synthesis of isolated core-shell Pt–ceria nano-catalyst is the maintenance of these particles against agglomeration, which is related to the surface charge on the ceria. The isoelectric point (zero point charge) of ceria is 8.1 ± 0.1 [26] which is much closer to the pH of the ammonia than the sodium hydroxide. Thus, agglomeration of nearly zero charged ceria particles prepared *via* ammonia solution could lead to phase segregation. As a result, sodium hydroxide is selected as the base for the microemulsion synthesis.

3.4. Effect of ageing time

Samples (5% platinum with ceria) prepared with different ageing times were tested towards WGS reaction. The results are shown in Fig. 6. From this figure, it is evident that the sample with 6 days

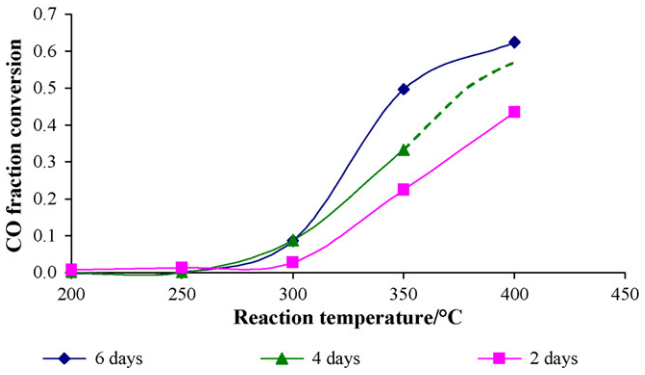

Fig. 6. A plot of CO fraction conversion towards WGS reaction vs. reaction temperature over Pt/CeO_2 catalysts prepared with different ageing times.

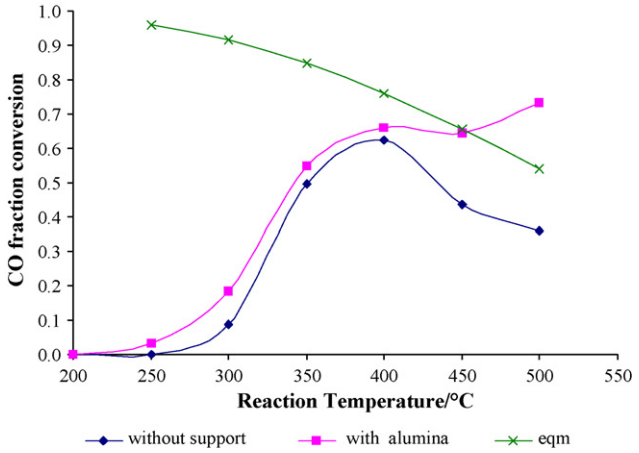

Fig. 7. A plot of CO fraction conversion vs. reaction temperature over Pt/CeO_2 catalysts with or without alumina support towards WGS reaction. The contents of CO, CH_4 and CO_2 were monitored during the catalytic test. There was 33.0% of carbon imbalance (compared with initial CO content in the feeds) recorded at 500 °C for the sample with alumina support used.

of ageing time gives a better activity than those of 2 and 4 days. On the other hand, there is no evidence of metal segregation from the core-shell geometry (no methane activity for all the samples). As a result, the beneficial effect of a long ageing time is not yet known. It is interesting to point out that UV–vis diffuse reflectance detected no band gap structure of the ceria samples with the 2- and 4-day ageing times but interestingly, the band absorption of ceria was clearly observed with the 6-day ageing time [21]. Thus, it is believed that longer ageing time may be required to create ceria over-layer with desirable electronic properties for the WGS reaction.

3.5. Effect of support used

The effect of adding a macroscopic support to disperse the catalyst nanoparticles on the overall catalytic WGS activity was studied in this work. The result is shown in Fig. 7. Two samples containing the same quantity of 5 wt% Pt/ceria prepared by microemulsion, one with and one without adding the Al_2O_3 support were tested for WGS reaction under the same reaction conditions as used before. From this figure, it is indeed found that the sample with a dispersion of nanoparticles on an alumina support gives a slightly high activity at comparable temperatures (clearly different at 300 °C). However, at above 400 °C the alumina supported samples showed deviation of their CO fraction conversions from equilibrium. It is well known that carbon deposition can take place on alumina from the WGS mixture over this temperature regime, and indeed, white powdered of the supported catalyst turned grey in color after the catalysis. As a result, both the beneficial and adverse effects on adding a macroscopic support material to the nano-catalysts can be clearly observed.

3.6. Effect of metal pre-reduction

It is established earlier that the sequential addition of a water-soluble Pt precursor followed by a ceria precursor into the reversed micelles during ME catalyst synthesis gives the best catalytic performance. This work was to investigate whether the pre-reduction of the platinum precursor in micelle using hydrazine hydrate before the application of the ceria precursor is important or not. As a result, two samples were tested in this experiment. One sample was pre-reduced using hydrazine hydrate before the ceria jacket formation, and the other one was prepared without the pre-reduction. In

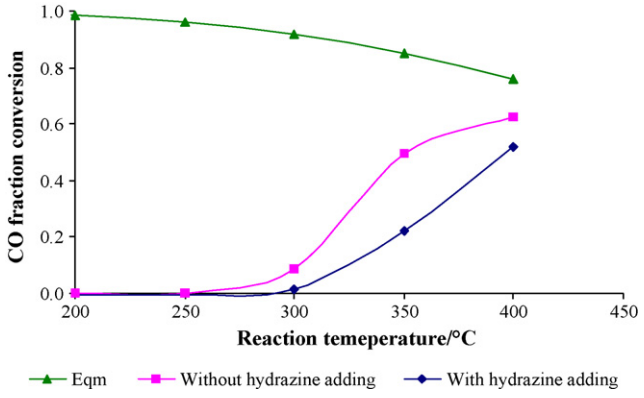

Fig. 8. A plot of CO fraction conversion vs. reaction temperature over 5 wt% Pt/CeO_2 catalysts with and without hydrazine hydrate treatment towards WGS reaction.

Fig. 8, it can be clearly seen that the material without the hydrazine hydrate treatment shows a higher activity towards the WGS reaction giving a lower onset temperature for CO conversion. Also, it is found that there was a mass imbalance during the catalysis in the case of sample with hydrazine hydrate treatment. Thus, it suggests that carbon deposition took place in this sample.

From the XRD analysis (Fig. 1) no platinum metal was detected from the sample without the hydrazine hydrate treatment indicative of Pt size smaller than 2 nm. However, the platinum metal peak was clearly identified from the sample with hydrazine hydrate treatment. The size of the platinum metal is estimated to be 10.8 nm by Scherrer equation, which is far larger than the micelle can accommodate for the given W ratio. It is therefore clear that the pre-reduction step by the hydrazine hydrate treatment will induce breakdown of the micelles causing metal agglomeration (formation of methane is also detected).

3.7. Effect of single metal doper

Different noble metals (Pt, Au and Pd) at the same 5 wt% loading were tested for the WGS reaction and the results are shown in Fig. 9. The figure clearly shows that Pt as the metal core appears to be much more active than the other metals. Pd/CeO_2 shows some degree of activity for the WGS at elevated temperatures. However, Au/CeO_2 displays no activity for the WGS reaction under the same reaction condition used before. This is somewhat surprising since the Au on ceria prepared by traditional methods such as

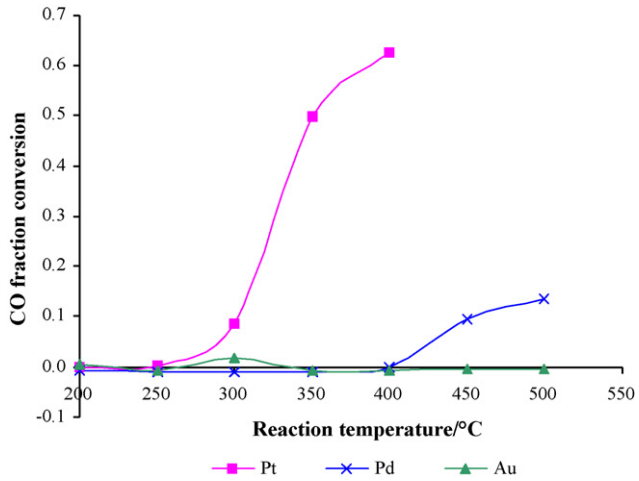

Fig. 9. A plot of CO fraction conversion vs. reaction temperature over ceria catalysts with different noble metals of same metal loading (5 wt%).

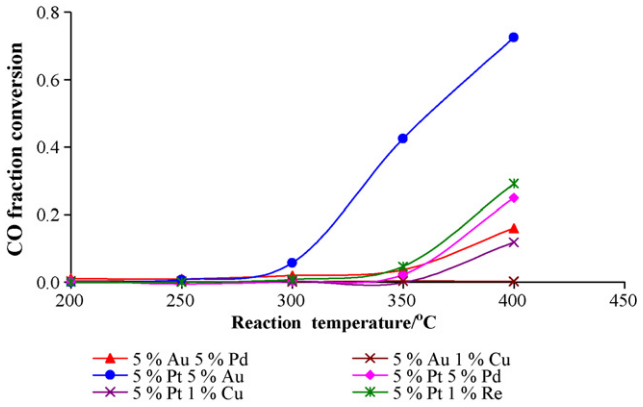

Fig. 10. A plot of CO fraction conversion vs. reaction temperature over two metal dopers with weight by percentage of metal doper used shown in the legend.

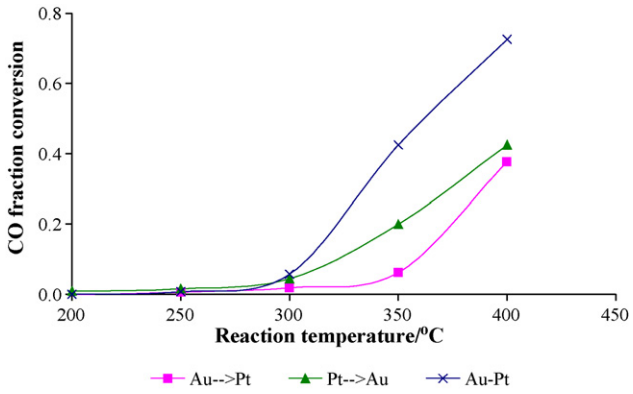

Fig. 11. A plot of CO fraction conversion vs. reaction temperature over $PtAu/CeO_2$ catalysts prepared by our microemulsion technique with different sequences of adding Au and Pt precursors.

co-precipitation is well known to give good WGS activity, particularly at the lower temperature regime (150–300 °C) [27,10]. The Au nanoparticle encapsulated in silica shown in Fig. 3 also showed no activity. This suggests that Au on ceria interface may catalyse WGS reaction under different mechanism as Au ion on ceria surface has been postulated to be the active phase [1]. The total encapsulation of Au by ceria may not be able to provide active sites for the catalysis.

3.8. Effect of two metal dopers (co-doping)

For a single metal core Pt appears to give the highest WGS activity. It would be interesting to see whether adding more than one metal in the micelle core could further improve the WGS activity. As a result, two aqueous metal precursors were added simultaneously into the reversed micelles, followed by adding NaOH and then ceria precursor. The catalytic results are summarised and shown in Fig. 10. From this figure, platinum–gold shows the best catalytic performance towards WGS reaction amongst all of the two metal dopers tested. Comparing to the data of MEs 5% Pt/ceria shown in the previous figure (Table 1), a higher WGS activity than the single Pt metal was also achieved (70.6% vs. 62.5% CO conversion at 400 °C). It is noteworthy that the activity of this Pt–Au catalyst differed significantly from the other Au-containing catalysts where Pd–Au catalyst showed a much lower activity, and the Cu–Au and pure Au metal catalysts were totally inactive (Fig. 10). For gold catalysts, it has been reported that their catalytic activity is very sensitive to their preparation method [28,29] depending on the choice of support and the architecture of the metal–support interaction. Even the temperature, pH, stirrer speed, feed flow rate, time of ageing, thermal treatment [30], etc., can exert strong influences on the structure hence the catalytic properties of the catalysts. Perhaps, the microemulsion method used in this work may not be a suitable method to prepare gold-based catalysts for the WGS reaction (unsure if the total encapsulation of gold metal in ceria is the right architecture of metal–support interaction). On the other hand, the Pt–Au core appears to be very unusual showing the highest WGS activity, which was therefore further optimized.

3.9. Effect of adding Pt and Au precursors in a sequential manner

Scheme 1 shows the envisaged geometry of a Pt–Au/ceria catalyst prepared using different procedures. One trial was to prepare the material *via* co-adding gold–platinum aqueous precursors, then adding the base to create a precipitate in the reversed micelle. The second trial involved adding platinum precursor, then the base followed by gold precursor and the third one, the gold precursor then the base followed by the platinum precursor. The last step of adding ceria precursor was identical for all the three materials.

As shown in Fig. 11, the catalyst synthesized *via* co-adding Pt–Au precursors into the reversed micelles gives a higher catalytic activity towards WGS reaction than the other two catalysts. It is believed that the formation of a Pt–Au alloy, which exerts the desirable electronic effect on the ceria over-layer for the WGS, might be involved [21]. However, it is rather difficult to prove the alloy formation at such small dimensions (no metal peaks from XRD). In addition, whether the formation of a truly homogeneous alloy at this 1:1 composition has occurred in the core of the nanoparticle is also uncertain, although thermodynamically the solubility of Au in Pt (and vice versa) is low. (Au is only soluble in Pt in the range of 1–2% and 86–100% of Au wt% compared to Pt [31].)

3.10. Effect of different ratio of Pt to Au metals loading in metal core

Following the same order of firstly adding Pt and Au precursors, secondly base and then ceria precursor, different molar ratios of Pt and Au were tested. Their catalytic activities are reported in Fig. 12. As seen from the figure, those samples with 5 wt% Pt loading appeared to be more active than that of 1 wt% Pt loading. As shown previously, 5 wt% Pt (as a single doper) displays a superior activity than 1 wt% Pt or Au alone which are not active at all over the whole

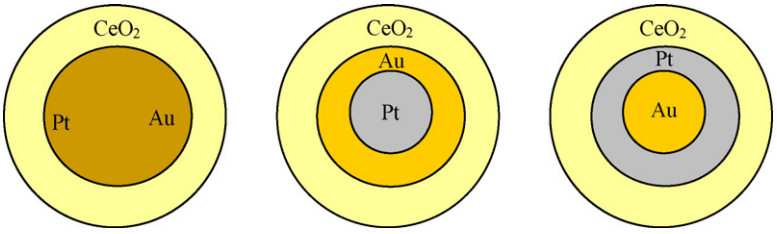

Scheme 1. Envisaged geometry of $PtAu/CeO_2$ catalysts synthesized by our microemulsion technique with different sequences of adding metal precursors.

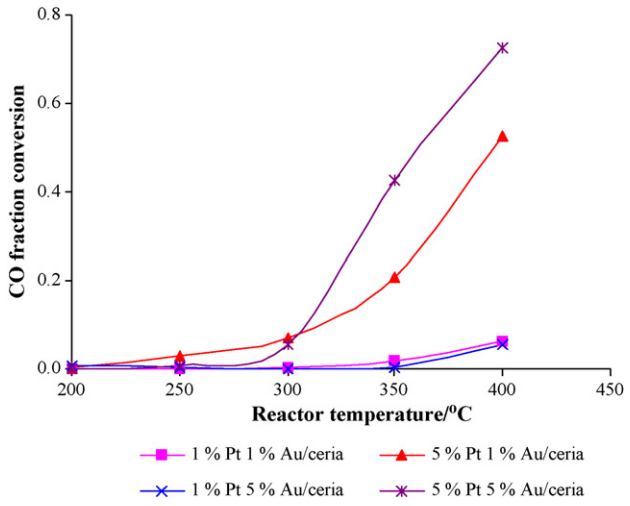

Fig. 12. A plot of CO fraction conversion vs. reaction temperature over $PtAu/CeO_2$ catalysts prepared by microemulsion technique with different Pt and Au loadings. The legends show the weight percent of Pt and Au metals in the catalysts.

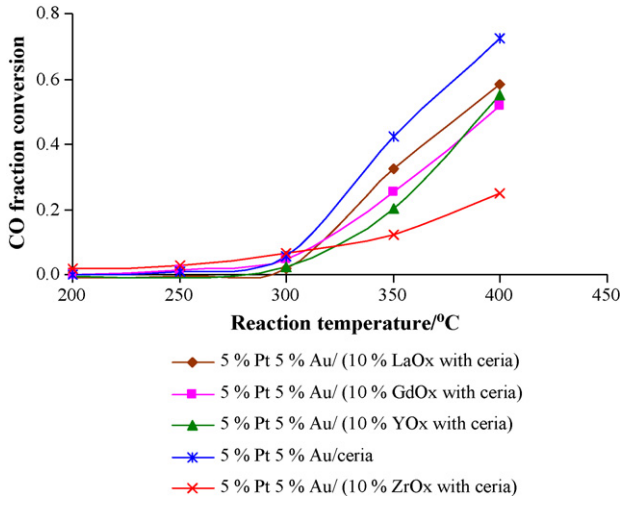

Fig. 13. A plot of CO fraction conversion vs. reaction temperature over 5 wt% Pt, 5 wt% Au with different composition of oxide over-layer. The oxide doper was kept at 10 mol% level on ceria in each case.

reaction temperature range tested [21,22]. Thus, the detection of some activity at elevated temperatures over the 1 wt% Pt–1 wt% Au and 1 wt% Pt–5% Au (Fig. 12) clearly suggest the beneficial effect of using two metals in the core. It is noted that there is a very similar atomic radius of Pt and Au of 1.83 and 1.79 Å, respectively; it is difficult to envisage that such a beneficial catalytic effect is related to their relative sizes. On the other hand, Pt and Au differ from each other by one atomic number so their electronic effect on WGS could be significant.

3.11. Different doper on ceria jacket ($PtAu/Ce_{0.9}M_{0.1}O_2$)

Oxygen storage capacity (OSC) and oxygen mobility of ceria are found to be crucial fundamental properties to its catalytic performance over a number of catalytic reactions [32–36]. It has been reported in the literature [37,38] that doping a rare earth metal oxide such as lanthanum oxide, yttrium oxide, gadolinium oxide, samarium oxide, praseodymium oxide, and zirconium oxide into ceria would improve the oxygen storage capacity (OSC) or oxygen mobility of the modified ceria. In addition, incorporation of zirconia to ceria has been reported to improve the thermal stability of the ceria against sintering [39,40]. As a result, different compositions of ceria over-layers on platinum–gold cores were prepared by the microemulsion technique and their catalytic activities are summarised in Fig. 13. The doping (lanthanum oxide, yttria, gadolinia, zirconia) was kept at 10 mol% with respect to the ceria content. Platinum and gold metal loadings were both kept at 5 wt%. From the activity evaluation, it was found that no improvement in activity was encountered despite the different oxide dopers incorporated. For catalysts with lanthanum oxide, yttrium oxide or gadolinium oxide as the doper, the catalytic activities towards WGS reaction were indeed less active compared to the pure ceria.

In contrast, the TPR data (Fig. 14 and Table 2) apparently suggested the doper improved the reducibility of catalysts. As noted from Fig. 14 there are mainly two reduction peaks associated with all ceria-based samples in their TPR spectra. Typically, for the pure ceria samples the two reduction peaks take place at around 450 and 850 °C (10 °C min^{-1} ramping, 30 mL min^{-1} flow of diluted H_2) which are attributed to the reductions of surface and bulk oxygen of ceria, respectively [7,41–45]. Fig. 14 and Table 2 clearly show that incorporation of the foreign oxide doper(s) into ceria can facilitate the reduction of surface oxygen of ceria at lower temperatures but the reduction of bulk oxygen in ceria seems unaltered. No correlation was found between the facilitated surface oxygen reductions by doper with the measured WGS activity.

It is known that pure CeO_2 has a fluorite structure with each Ce^{4+} cation octahedrally coordinated to eight equivalent O^{2-} ions and each O^{2-} anion tetrahedrally coordinated to four Ce^{4+} ions. Doping of rare earth metal oxide to ceria should result to replace Ce centres with the doping metal ion in a random solid solution [38,46–48]. Depending on the size of the doping metal ion, a degree of structural perturbation to the lattice of ceria can result. The sizes of yittrium (Y^{3+}, 1.02 Å) and gadolinium (Gd^{3+}, 1.05 Å) are comparable to the size cerium ions (Ce^{4+}, 0.97 Å) [49] which are expected to induce the lesser structural perturbation to the ceria lattice. It is interesting that these two metal oxide dopers gave a slightly lower catalytic activity towards WGS reaction as compared to undoped ceria. It is therefore concluded that the overall catalytic WGS activity of these NM/ceria-based catalysts could relate to the structural aspects of ceria rather than to their oxygen mobility and OSC properties. In addition, the band gap (from the absorption edge of O_{2p}–Ce_{4f}) of the n-type semiconducting ceria was estimated using UV–vis diffuse reflectance measurement over this series of ceria-based catalysts. From the diffuse UV reflectance, red shifts in the order of doper, La,

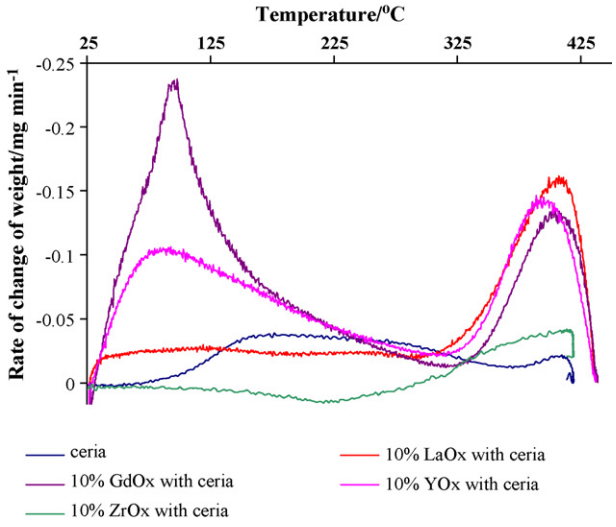

Fig. 14. H_2-TPR profiles of 5 wt% Pt, 5 wt% $Au/Ce_{0.9}Ln_{0.1}O_2$ catalysts promoted with a different lanthanium metal oxide (measured by gravimetric means).

Table 2
H_2-TPR results for 5 wt% Pt, 5 wt% Au/$Ce_{0.9}Ln_{0.1}O_2$ catalysts promoted with a different lanthanium metal oxide.

Doper	First peak max (°C)	Second peak max (°C)	Third peak max (°C)	Fourth peak max (°C)
None	177		408	
Lanthanum oxide	124	254	413	
Yttrium oxide	91		401	
Gadolinium oxide	98		409	
Zirconium oxide	143	303	418	453

Table 3
UV–vis diffuse reflectance measurements for 5 wt% Pt, 5 wt% Au/$Ce_{0.9}Ln_{0.1}O_2$ catalysts promoted with a different lanthanium oxide.

Doper	Band transition energy/eV	Difference/eV[a]
None	3.3374	–
Lanthanum oxide	3.3077	0.0297
Yttrium oxide	3.2906	0.0468
Gadolinium oxide	3.2596	0.0778
Zirconium oxide	3.2475	0.0899

[a] Difference in band transition energy compared to the 5 wt% Pt, 5 wt% Au/CeO_2.

Y, Gd and Zr were observed. These distortions of the band structure are thought to relate to the structural modifications as mentioned above where La and Y did not induce much red shift in the absorption edge of O_{2p}–Ce_{4f}. Interestingly, the WGS activity evaluation of this series followed inversely the order of the red shift at 400 °C (Fig. 13).

Our earlier communication suggests that a possible electron transfer mechanism may take place at the interface between ceria and metal (with a higher work function) *in facilitating the redox properties of the ceria* [21]. As a result, a progressive enlargement in band gap of O_{2p}–Ce_{4f} by metal doper will give a higher WGS activity. As seen from Table 3, doping lanthanium oxide, in the contrary, decreases this band gap giving lower WGS activity hence this trend agrees very well with the proposed electronic transfer mechanism.

4. Conclusion

The main research activity in searching new WGS catalysts in this area in the literature has been on applying the WGS reaction to produce hydrogen for mobile fuel cells applications, especially for automobile industry. As a result, the interested temperature should be as close as the fuel cells operation temperatures (80–100 °C) for efficient heat management. But this interest has been greatly attenuated due to the fact that most car companies have opted for hydrogen storage (hydrogen production from factory) to supply fuel cells vehicles. As stated in the introduction, we were not only interested in mobile applications but also stationary applications for hydrogen production at small scale for chemical synthesis. Thus our interested temperature range was from 80 to 450 °C. Our industrial partner laboratory (JM) has shown that the Pt/CeO_x samples of different composition in the temperature regime of 300–450 °C can outperform typical low temperature WGS Cu/ZnO catalysts in term of activity (also shown in Table 1). From the catalytic testing, the new class of microemulsion prepared NM/ceria catalysts particularly shows even higher catalytic activity towards WGS reaction than those Pt/CeO_x catalysts prepared by traditional methods under the high temperature regime (Table 1). This type of catalyst also displays some unusual but unique properties such as the inhibition of methane formation where the production of methane is thermodynamically favorable in the presence of carbon oxides and hydrogen at elevated temperatures. Thus, this new type of catalysts seems to be more appropriate for the high temperature stationary applications rather than the low temperature mobile applications where their catalytic activity appears to be insufficient at <300 °C. It is therefore justified to further investigate some synthesis details of this new method as for the development of new WGS catalysts for the high temperature stationary applications.

We have recently carried out an extensive study on testing, characterization and reaction mechanism elucidation of these new microemulsion prepared NM/ceria catalysts [50]. The results clearly suggest that small metal atoms/ions are embedded in a thin ceria oxide coat of controllable dimension in the microemulsion catalysts. By eliminating the exposed metal sites on ceria, this new type of catalysts is still capable of giving a high WGS activity. As stated in this study, Pt dispersion of the microemulsion Pt/ceria was extremely lower than that of the catalyst prepared by co-precipitation, but it exhibited superior WGS activity than that of the co-precipitation catalyst. We have attributed to the electronic effect exerted from enclosed metal to the surrounding high surface area cerium oxide which provides exclusively all active sites for WGS [50]. In the WGS reaction, there is no agreement on the nature of the active site over conventional Pt on ceria catalysts, the conclusions of which could depend on particular reaction conditions used. For example, Gorte [51] propose exposed NM sites on the surface of ceria to be crucial to shift activity, Flytzani-Stephanopoulos [1] attributes to the ionic Pt in ceria and ceria sites promoted by metal has also been proposed. Although it should be emphasised that the relative significance of this kind of observed catalysis over ceria encapsulated metal samples compared to those of traditional exposed metal–ceria interface is not yet known, but the unusual metal–metal oxide encapsulation geometry in this new class of microemulsion catalysts has clearly shown to display superior catalytic properties over the current catalyst systems (higher activity and unselective to methane formation at elevated temperature) for WGS.

Empirical optimizations of this type of catalyst in a number of synthetic parameters have therefore been studied systematically with respect to their overall catalyst WGS activity in this paper. It is found that the sequence of adding chemical precursors into the micelle is very important with regards to the geometry of the resulting material and hence the activity of the catalyst. The initial establishment of precipitation of water-soluble noble metal precursors in micelles followed by polymerization of cerium hydroxyl precursors can give an active catalyst precursor. Amongst some typical noble metals (Pt, Pd, Au, Cu), Pt is found to be the most effective metal as the core in these core-shell NM/ceria catalysts. On the other hand, an Au metal core encapsulated in ceria is found to be totally inactive for the WGS reaction, which appears to contradict the claim of exceptionally high activity of Au/ceria in the literature [27,10]. This may reflect that the core-shell architecture of the Au/ceria prepared by our microemlusion method is not the appropriate morphology for WGS in the case of Au–ceria system. On the other hand, a bimetallic core of Pt and Au in a 1:1 ratio at 5 wt% with respect to the ceria shell is found to show the highest WGS activity. Although there is no direct evidence of alloy formation (Pt–Au) a highest band transition shift by this bimetallic core to the ceria is noted [21].

Doping of rare earth metal oxide to the ceria coating in the platinum–gold encapsulated does not result in a higher WGS activity, though the promotion by this foreign oxide (rare earth metal oxide) can significantly improve the reducibility of surface oxygen on ceria at much lower temperatures. On the other hand, the order

of the WGS activity over these doped materials follows inversely the extent of the red shift in their diffuse UV reflectance measurements. These distortions to the electronic band structure of ceria are thought to relate to the structural modifications by rare earth oxide promotion. It is therefore concluded that the overall catalytic WGS activity of these NM/ceria-based catalysts could relate to the structural/electronic aspects of ceria instead of their oxygen mobility and OSC properties in this new type of catalysts.

Acknowledgments

We are grateful to the EPSRC and Johnson Matthey, plc of UK for supporting this work.

References

[1] Q. Fu, H. Saltsburg, M. Flytzani-Stephanopoulos, Science 301 (2003) 935.
[2] D. Tibiletti, A. Goguet, F.C. Meunier, J.P. Breen, R. Burch, Chem. Commun. 14 (2004) 1636.
[3] G. Jacobs, L. Williams, U. Graham, D. Sparks, B.H. Davis, J. Phys. Chem. B 107 (2003) 10398.
[4] A.F. Ghenciu, Curr. Opin. Solid State Mater. Sci. 6 (2002) 389.
[5] T. Shido, Y. Iwasawa, J. Catal. 136 (1992) 493.
[6] C. Hardacre, R.M. Ormerod, R.M. Lambert, J. Phys. Chem. 98 (1994) 10901.
[7] S.E. Golunski, H.A. Hatcher, R.R. Rajaram, T.J. Truex, Appl. Catal. B: Environ. 5 (1995) 367.
[8] S. Velu, K. Suzuki, M. Okazaki, M.P. Kapoor, T. Osaki, F. Ohashi, J. Catal. 194 (2000) 373.
[9] F. Joensen, J.R. Rostrup-Nielsen, J. Power Sources 105 (2002) 195.
[10] Q. Fu, S. Kudriavtseva, H. Saltsburg, M. Flytzani-Stephanopoulos, Chem. Eng. J. 93 (2003) 41.
[11] D.S. Kalakkad, A.K. Datye, H.J. Robota, J. Catal. 148 (1994) 729.
[12] H.S. Ghandi, M. Shelef, Stud. Surf. Sci. Catal. 30 (1987) 199.
[13] M.K. Ozawa, J. Mater. Sci. Lett. 9 (1990) 291.
[14] A. Trovarelli, Catal. Rev. Sci. Eng. 38 (4) (1996) 439.
[15] K. Li, Q. Fu, M. Flytzani-Slephanopoulos, Appl. Catal. B: Environ. 27 (2000) 179.
[16] W. Ruettinger, O. Ilinich, R.J. Farrauto, J. Power Sources 118 (2003) 61.
[17] S.L. Swartz, Proceedings of the Fuel Cell Seminar, Palm Springs, USA, 2002, p. 587.
[18] Q. Fu, A. Weber, M. Flytzani-Stephanopoulos, Catal. Lett. 77 (2001) 87.
[19] H. Sakurai, T. Akita, S. Tsubota, M. Kiuchi, M. Haruta, Appl. Catal. A 291 (2005) 179.
[20] M. Fowler, private communication (Johnson Matthey).
[21] C.M.Y. Yeung, K.M.K. Yu, Q.J. Fu, D. Thompsett, M.I. Petch, S.C. Tsang, J.A.C.S. 127 (2005) 18010.
[22] C.M.Y. Yeung, F. Meunier, R. Burch, D. Thompsett, S.C. Tsang, J. Phys. Chem. B 110 (2006) 8540.
[23] N.A. Zhilyaeva, E.A. Volnina, M.A. Kukina, V.M. Frolov, Petrol. Chem. 42 (6) (2002) 367.
[24] K.M.K. Yu, D. Thompsett, S.C. Tsang, Chem. Commun. 13 (2003) 1522.
[25] K.M.K. Yu, C.M.Y. Yeung, D. Thompsett, S.C. Tsang, J. Phys. Chem. B 107 (19) (2003) 4515.
[26] L. Defaria, S. Trasatti, J. Colloid Interface Sci. 167 (2) (1994) 352.
[27] D. Andreeva, V. Idakiev, T. Tabakova, L. Ilieva, P. Falaras, A. Bourlinos, A. Travlos, Catal. Today 72 (2002) 51.
[28] G.C. Bond, D.T. Thompson, Gold Bull. 33 (2000) 41.
[29] G.C. Bond, D.T. Thompson, Catal. Rev. Sci. Eng. 41 (1999) 319.
[30] D. Andreeva, Gold Bull. 35 (3) (2002) 82.
[31] G. Schmid, Chem. Rev. 92 (1992) 1709.
[32] M.S. Dresselhaus, I.L. Thomas, Nature 414 (2001) 332.
[33] T. Hibino, A. Hashimoto, T. Inoue, J. Tokuno, S. Yoshida, M. Sano, Science 288 (2000) 2031.
[34] S.D. Park, J.M. Vohs, R.J. Gorte, Nature 404 (2000) 265.
[35] B.C.H. Steele, A. Heinzel, Nature 414 (6861) (2001) 345.
[36] N.V. Skorodumova, S.I. Simak, B.I. Lundqvist, I.A. Abrikosov, B. Johansson, Phys. Rev. Lett. 89 (2002) 166601.
[37] G.B. Balazs, R.S. Glass, Solid State Ionics 76 (1995) 155.
[38] G. Liu, J.A. Rodriguez, J. Hrbek, J. Dvorak, C.H.F. Peden, J. Phys. Chem. B 105 (32) (2001) 7762.
[39] M. Pijolat, M. Prin, M. Soustelle, O. Touret, P. Nortier, J. Chem. Soc. Faraday Trans. 91 (1995) 3941.
[40] A. Holmgren, B. Andersson, D. Duprez, Appl. Catal. B: Environ. 22 (1999) 215.
[41] H.C. Yao, Y.F.Y. Yao, J. Catal. 86 (1984) 254.
[42] B. Harrison, A.F. Diwell, C. Hallett, Platinum Met. Rev. 32 (1998) 73.
[43] A.F. Diwell, R.R. Rajarama, H.A. Shaw, T.J. Truex, Stud. Surf. Sci. Catal. 71 (1991) 139.
[44] M.F.L. Johnson, J. Mooi, J. Catal. 103 (1987) 502.
[45] V. Perrichon, A. Laachir, G. Bergeret, R. Frety, L. Tournayan, O. Touret, J. Chem. Soc. Faraday Trans. 90 (1994) 773.
[46] S. deCarolis, J.L. Pascual, L.G.M. Pettersson, M. Baudin, M. Wojcik, K. Hermansson, A.E.C. Palmqvist, M. Muhammed, J. Phys. Chem. B 103 (1999) 7627.
[47] M. Luo, J. Chen, L. Chen, J. Lu, Z. Feng, C. Li, Chem. Mater. 13 (2001) 197.
[48] G. Vlaic, R. DiMonte, P. Fornasiero, E. Fonda, J. Kaspar, M. Graziani, J. Catal. 182 (1999) 378.
[49] R.D. Shannon, Acta Crystallogr. A32 (1974) 751.
[50] C.M.Y. Yeung, S.C. Tsang, J. Phys. Chem. C 113 (2009) 6074–6087.
[51] G. Jacobs, P.M. Patterson, L. Williams, E. Chenu, D. Sparks, G. Thomas, B.H. Davis, Appl. Catal. A: Gen. 262 (2004) 177.